JOURNAL OF AIRCRAFT
Vol. 39, No. 6, November–December 2002

Jig-Shape Static Aeroelastic Wing Design Problem: A Decoupled Approach

Sherif Aly*
PTC Global Services, Parsippany, New Jersey 07054
Madara Ogot† and Richard Pelz‡
Rutgers University, Piscataway, New Jersey 08854
and
Mike Siclari§
Northrup Grumman Corporation, Bethpage, New York 11714-3580

A novel approach to the jig-shape static aeroelastic wing design problem is presented in this paper. Unlike previous design efforts where the aerodynamic and structural analyses were coupled throughout the optimization process, this work presents a truly decoupled approach. The proposed approach performs aerodynamic shape optimization in the first phase to determine an optimal configuration, followed by structural shape optimization in the second phase to find the corresponding jig shape. The latter does not require the performance of any new aerodynamic analyses, resulting in true decoupling of the jig-shape aeroelastic wing design problem. This results in significant reduction in computation time making the design of relatively complex wing structures feasible. For this study high-fidelity codes—ANSYS 5.0 for the structural analyses and a supersonic Euler code for the aerodynamic analyses—were used. A modified simulated annealing algorithm was used as the optimizer. Two examples are presented a forebody problem and the design of a high-speed civil transport wing, to demonstrate the efficacy of the methodology.

Nomenclature

r	=	cross-sectional radii
S_{ad}	=	actual deflected shape
S_{dd}	=	desired deflected shape
S_{ud}	=	desired undeflected shape
t	=	shell thickness
z	=	z-station location
ΔA	=	actual maximum nodal deflection
ΔD	=	desired maximum nodal deflection
δ_i	=	structural error, difference between desired and actual nodal location

Introduction

THE design of modern, high-speed performance aerospace vehicles is characterized by unprecedented levels of multidisciplinary interactions of a number of technical disciplines such as structures, aerodynamics, controls engineering, and manufacturing. These disciplines, among others, can impose considerable constraints on the dynamic stability and controls performance margins required for flight safety.

One of the many phenomena that exists in complex aircraft design is aeroelasticity: the study of the mutual interaction among inertial, elastic, and aerodynamic forces. The role of aeroelasticity in the design cycle for high-performance aircraft was realized as far back as the early 1970s during the early years of the U.S. Supersonic Transport program. It was then concluded that major configuration design decisions such as the placement of the wing on the body and the type and weight of various structural areas are paced by the engineering efforts involved in structural analyses.[1]

The tradeoff between low drag and low structural weight for an aircraft is primarily affected by two means of interaction between the aerodynamic and structural response. An increase in the structural weight results in an increase in the required lift and therefore higher forces of induced drag. On the other hand, the aerodynamic forces acting on the aircraft cause structural deformations that change the aerodynamic shape and adversely affect the performance. One solution is to increase the stiffness of the structure in order to minimize deformations. However, this results in an increase in weight that degrades overall performance because of the requirement of more lift. An alternative solution compensates for this effect by designing the structure such that the structural deformation, caused by the aerodynamic forces, results in the desired aerodynamic shape. This so-called jig-shape approach accounts for the deformations of the aircraft structure[2] and is the focus of this paper.

The jig-shape approach to wing design is applicable to cases with primarily static aeroelastic effects yielding wing deformations that are approximately constant through most of the flight time. This is the case for many transports that spend most of their flight time at cruise conditions. However, this approach might be ineffective in the design of aircraft wings across their total flight time—takeoff, cruise, and landing—because an aircraft undergoes a variety of loading conditions.

If the effects of structural deformation on aerodynamic performance can be corrected by the jig shape, the interaction between the aerodynamics and structures becomes unidirectional. The aerodynamic design affects all of the aspects of the structural design, whereas the structural design affects the aerodynamic design primarily through structural weight. The unidirectionality permits static aeroelastic problems to be treated as two level optimization problems, with the aerodynamic problem at the upper level and the structural design at the lower level.[2–4] Taking advantage of the asymmetric interaction between the structures and aerodynamics presents an enormous potential for savings in computational resources.

Received 11 February 2001; revision received 16 July 2002; accepted for publication 18 August 2002.

*Consultant.
†Associate Professor, Department of Mechanical and Aerospace Engineering, 98 Brett Road.
‡Professor, Department of Mechanical and Aerospace Engineering, 98 Brett Road. Senior Member AIAA.
§Principal Engineer. Associate Fellow AIAA.

Previous Research on the Jig-Shape Problem

A jig-shape approach for the aerodynamic and structural optimization of the high-speed civil transport (HSCT) was presented by Rohl et al.[5] They incorporated several approximation tools in the determination of an undeformed wing shape that deforms into its cruise shape under the cruise load condition. The procedure to determine the wing jig shape was initiated by the Flight Optimization System code,[6] which produced a baseline configuration. For the wing planform and cruise condition of this design, the wing design program, WINGDES, was run to determine the optimum twist and camber distribution. The latter was superimposed over the "flat" wing grid that the Automated Structural Optimization System (ASTROS) preprocessor had produced. This yielded the final cruise shape into which the wing was supposed to deform. ASTROS is a multidisciplinary design tool capable of incorporating static, dynamic, aerodynamic, aeroelastic, and aeroservoelastic disciplines for analysis and optimization of finite element models.[7]

Several areas of the jig-shape approach proposed in Rohl et al.[5] are further investigated in the present study. Although they decomposed the wing structural design problem into three hierarchical levels, the structural and aerodynamic analyses were not completely decoupled. During the structural shape optimization, both the aerodynamic and structural analyses were performed iteratively to solve the aeroelastic problem. Further, low-fidelity approximation techniques were employed at every level of the design problem. Although approximation methods play a significant role in the preliminary design process, higher fidelity codes are needed to provide more accurate detailed analyses of aeroelastic phenomena. It is therefore necessary to develop a procedure utilizing advanced computational methods for both the aerodynamic and the structural disciplines.

A methodology performing structural optimization with static aeroelastic considerations was proposed by Karpel et al.[8] They incorporated aeroelastic effects into a nonlinear aerodynamic code originally developed to solve Euler or Navier–Stokes equations for a fixed shape configuration. Computational efficiencies are achieved through simultaneous convergence of the aerodynamic loads and the structural design. Karpel et al.[9] developed a multidisciplinary design optimization (MDO) approach to the static aeroelastic wing design problem by coupling the aerodynamic optimization with structural optimization as a suboptimization problem. This reduces the complexity of the MDO and simplifies the transfer of data from one discipline to the other. Other researchers have proposed modal-based aeroelastic optimization methods for static aeroelasticity. These methods utilize reduced-size models with low-frequency normal modes of the baseline structure as fixed coordinates throughout the optimization process, accelerating convergence to the optimal design.[10,11] A variable-complexity-modding design strategy combining aerodynamic and structural optimization was presented by Neill and Herendeen.[12] Their approach was applied to the HSCT.

Previous approaches to the jig-shape problem, as shown in the literature review, performed aerodynamic and structural analyses iteratively to solve the static aeroelastic problem. This paper presents a truly decoupled approach to the jig-shape aeroelastic wing design problem. In this study only aerodynamic analyses are performed during the aerodynamic shape optimization, and only structural analyses are performed during the structural shape optimization, thereby considerably reducing the computational requirements. The use of a stochastic optimizer overcomes the primary problem experienced by gradient-based optimizers: convergence to local minima. The efficacy of the methodology is demonstrated on two problems: to the aeroelastic design of a forebody and to the design of a wing for the HSCT.

Proposed Decoupled Approach

Aerodynamic and Structural Decoupling

The proposed jig-shape approach involves the following three steps:

1) Perform an aerodynamic shape optimization to determine the "optimal" shape by minimizing some performance criteria, for example, drag. This shape is referred to as the desired deflected shape S_{dd}.

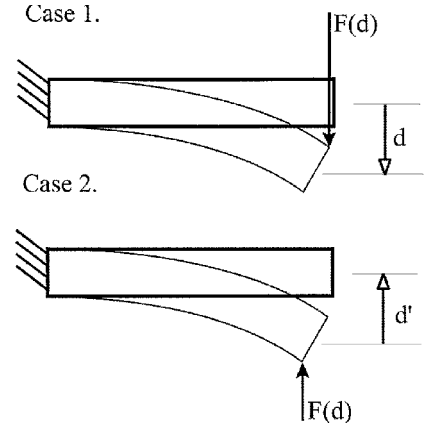

Fig. 1 Beam deflection analogies employed in the jig-shape structural shape optimization problem.

2) Using the final aerodynamic loading information determined in step 1, perform a structural shape optimization to determine an initial shape and object thickness that will deform into the S_{dd} on loading. As will be explained shortly, no new aerodynamic analyses are required.

3) Using the aerodynamic information determined in step 1, perform a modified structural shape optimization to refine the initial undeformed shape found in step 2. The shape from this step is referred to as the desired undeflected shape S_{ud}. As in step 2, no new aerodynamic analyses are required.

Step 1, the aerodynamic shape optimization, has been well documented in previous papers.[13,14] This paper will therefore focus on how the structural shape optimization can be performed (steps 2 and 3) without the need for new aerodynamic analyses. Throughout the discussions that follow, therefore, it will be assumed that the aerodynamic analyses have been completed.

The ability to decouple the problem can be explained via the beam analogy illustrated in Fig. 1. Consider the two cases contained therein:

1) A beam is subject to a load $F(x)$, whose magnitude is dependent on the beam displacement x (similar to the aeroelastic problem). For a final displacement d the final applied load is $F(d)$. This corresponds to the end of the aeroelastic shape optimization described in step 1. The deflected beam shape and $F(d)$ correspond to S_{dd} and the final aerodynamic loading conditions, respectively.

2) Consider an undeflected beam whose shape is similar to the final deflected shape in case 1. By applying the final loading condition $F(d)$ in the reverse direction, a displacement d' is attained bringing the deflected beam shape close to the undeflected beam shape in case 1. Similarly, for the structural shape optimization the initial design S'_{ud} is determined by reversing the desired aerodynamic loads direction on an unstressed shape similar to S_{dd}.

Reapplying the final loading conditions on the initial design S'_{ud} does not result in a deflection to the S_{dd}. This is because the differences in displacements and stresses in a curved beam compared to a straight beam under similar loading conditions. S'_{ud}, however, is expected to be in the neighborhood of the final design. Confining the design space around this point reduces the overall computation time.

Once the initial design is determined, the desired body loading is applied, and a new deflected shape is calculated. The objective function for the shape optimization is defined as the L_p norm difference between the S_{dd} and the actual deflected shape S_{ad} of the current design (Fig. 2). As the optimization proceeds, the average difference between S_{dd} and S_{ad} is driven towards zero, yielding S_{ud}.

Interfacing Aerodynamic and Structural Analyses

The coupling of aerodynamic and structural disciplines is accomplished by exchanging data at the interfaces between fluids and structures. This allows one to take full advantage of the numerical procedures for the individual disciplines such as finite volumes methods for fluids and finite element methods for structures. All

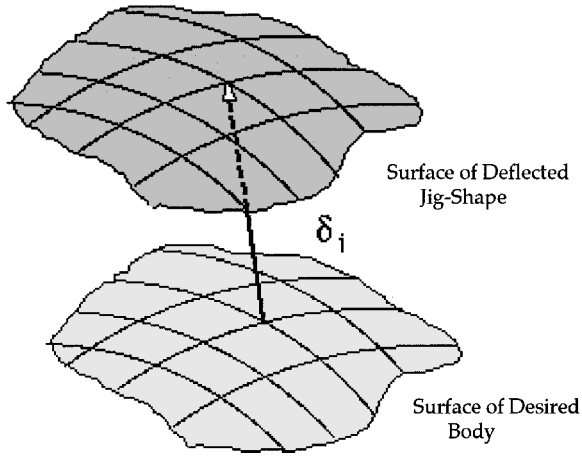

Fig. 2 Definition of δ_i used to determine the objective function of the structural optimization.

aeroelastic computations require that pressure loads be transmitted from the fluid dynamics side of the fluids/structures interface to the structural nodes on the other side of the interface. In general, the fluid and structure meshes have two independent representations of the physical fluids/structures interface.[15] When these representations are identical, that is, when every fluid point on the surface is also a structural node and vice versa, the evaluation pressure forces and the transfer of the structural motion to the fluid mesh becomes trivial.

However, typical analyses involve fluid and structure meshes that have different elements and have been independently created, refined, and validated. The following two problems must therefore be addressed: 1) when the fluid structure interfaces are not identical, their discretizations do not coincide and must therefore be "matched," and 2) the locating of specific points in the respective meshes, that is, fluid interface points must be located in the structure mesh and vice versa.[16]

Several different techniques have been suggested for the data exchange at the fluid and structure mesh interface. Blair[17] proposed an s-element, a simple linearized shell element based on a parametric bicubic surface spline, to promote a unified computational fluid dynamics (CFD)/computational structural mechanics surface formulation. Before initiating the aeroelastic process, Bhardwaj et al.[18] created mappings that transfer pressures on the fluids grid to the structural finite element grid and the resulting displacements on the finite element grid back to the fluids grid to deform it. The mapping only required the fluid surface and finite element grid point coordinates.

A method for sharing CAD geometry at the fluids/structures interface was presented by Samareh.[19] Once the CAD geometry was built, it was stored as a set of nonuniform rational B-splines shared by each discipline. Gupta[20] employed the finite element method (FEM) to model both the fluids and structures continua. The contributions of the aerodynamic nodal values to the structural node were computed by standard finite element interpolation procedures and element shape functions. Newman et al.[21] modeled the fluids/structures interface by generating the surface structural nodes for the finite element model as a subset of the aerodynamic surface grid. The interaction between the fluids and the structure was accomplished by lumping the aerodynamic forces at the surface structural nodes and applying them directly to the jig shape, that is, the unloaded wing shape.

A parallel grid-to-element approach was developed by Byun and Guruswamy[22] to define the location of the points of the fluid grid relative to the finite elements at the surface of the structure. In this approach every fluid grid point that lies on the fluids/structure interface was identified with respect to a finite element. Maman and Farhat[16] also developed a parallel approach to interfacing the fluids and structures meshes. They generated data structures needed for handling arbitrary and nonconforming fluids/structure interfaces in aeroelastic computations. An assessment of the performance of numerous approaches using nonlinear CFD methods coupled with linear representations of computational structural dynamics equations can be found in Smith et al.[23]

All of these formulations transfer data back and forth between the fluids and structural domains by the necessity of interactively performing both fluids and structural analyses. Removal of the aerodynamic analyses during the structural shape optimization, as presented in this paper, eliminates the need for bidirectional data transfer between the fluids and structural grids. Such a transfer is therefore only required for the aeroelastic verification of the final design.

For this study a very efficient hybrid finite volume implicit Euler marching method[24,25] was used for the aerodynamic analyses. The numerical formulation was based on the node-centered scheme developed originally by Jameson and is currently in use by NASA Langley to evaluate the HSCT configurations.[26]

ANSYS,[27] a commercial finite element code, was used for the structural shape optimization. The p-method, which provides an excellent way to solve a problem to a desired level of accuracy while using a coarse mesh, was utilized. The p-method manipulates the polynomial level (p-level) of the finite element shape functions that are used to approximate a real solution. The higher the p-level, the better the finite element approximation of the true solution is. Structural shell elements that support a polynomial with a maximum order of eight were used. They are particularly well suited to modeling curved shells. The elements are defined by eight nodes—one at each corner and one at each midside—and four thicknesses defined at each corner.

Shape Optimization Formulation

In general, the objective function can be formulated as

$$\min f_1 = \left(\frac{1}{n} \sum_{i=1}^{n} \delta_i^p \right)^{1/p} \tag{1}$$

subject to a maximum specified deflection and bounds on the design variables. In Eq. (1) f_1 is the average difference, structural error, at each of the nodal locations, δ_i is the geometrical difference between the actual and desired ith nodal location, and p represents the order of the normalization used. Increasing the value of p in the normalization magnifies the effects of the larger nodal geometrical differences in the objective function.

For this study the bodies were assumed to be shells of uniform thickness t. Because the value of t is unknown a priori, it is treated as an additional design variable. The value of the thickness primarily affects the magnitude of the nodal deflections obtained from the loading of the shell. To find the appropriate t that results in a desired maximum nodal deflection, the objective function f_1 is modified to

$$\min f_2 = W_1 \left(\frac{1}{n} \sum_{i=1}^{n} \delta_i^p \right)^{1/p} + W_2 |\Delta_D - \Delta_A| \tag{2}$$

where W_1 and W_2 are weighting factors. Minimization of f_2 yields the desired jig shape while meeting the maximum deflection requirement.

Simulated annealing, a stochastic optimization method, was used to perform the optimization. The next section presents two examples that demonstrate the efficacy of the proposed jig-shape approach. The first, design of a forebody, serves as a proof-of-concept. The second is the design of an HSCT wing.

Examples

Proof-of-Concept: Forebody Problem

This example focused on the geometry determination of an axisymmetric forebody for minimum drag, taking into account static aeroelastic effects, namely, structural deflection caused by aerodynamic loading. The body shape was defined at n equally spaced cross sections between the nose and the end of the forebody where a radius r_i is specified (Fig. 3). By fitting cubic splines between

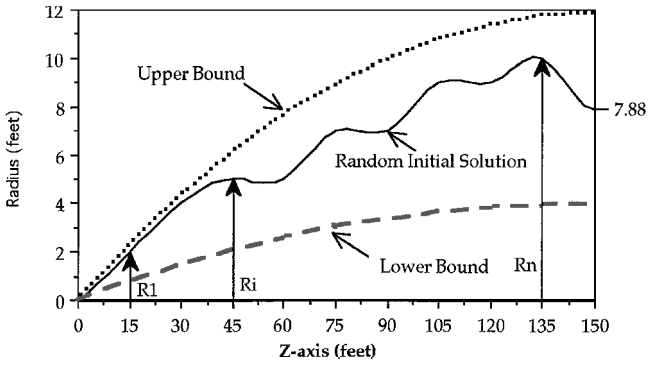

Fig. 3 Geometric definition of forebody profile. Cross-section radii defined at *n* stations equally spaced along the *z* axis.

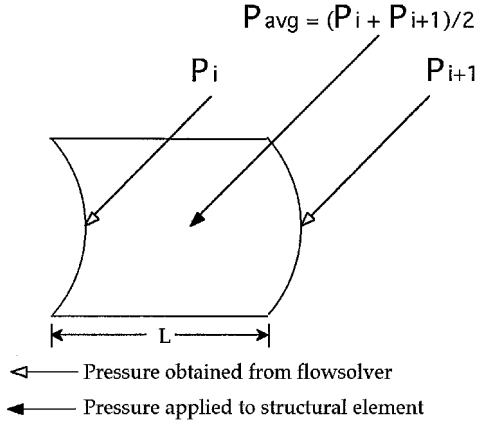

Fig. 4 Translation of aerodynamic loads to ANSYS finite elements.

the radii while enforcing an equal slope constraint between successive splines, the forebody profile was generated. A full rotation of the profile created the three-dimensional forebody shape. The aerodynamic shape optimization was previously documented in Aly et al.[14]

The generalized objective function presented in Eq. (2) took on the form in Eq. (3), where the structural error δ_i was measured at 50 equally spaced positions along the length of the body. For this problem the body was defined at 10 different cross sections. The locations of the cross sections (z_i) and the corresponding radii (r_i), coupled with the unknown shell thickness t, constituted the 21 design variables.

$$\min f_2(r, z, t) = W_1 \left(\frac{1}{50} \sum_{i=1}^{50} \delta_i^2 \right)^{\frac{1}{2}} + W_2 |\Delta_D - \Delta_A| \qquad (3)$$

Care was taken to ensure accurate translation of the desired aerodynamic loading onto the finite element mesh. The flow solver was set to yield aerodynamic pressures at 3-ft intervals along the z axis, coinciding with the boundaries of the finite elements (Fig. 4). The average pressure on each element P_{avg} was computed by averaging the two boundary pressures P_i and P_{i+1}. The interior of the body was assumed to be under freestream pressure.

The aerodynamic calculations were carried out on a relatively coarse mesh consisting of 39 circumferential and 40 radial cross-flow mesh points of the first conical mesh at 50 streamwise locations. This mesh was selected as it gave accurate results without excessive memory requirements or computation time. Flow solves were terminated when the final tolerance on the flow variable residual reached 0.001. Increasing the convergence tolerance by two orders of magnitude more than doubled the computation time required for one function evaluation.

Flight conditions were supersonic at Mach 2.4, with zero angle of attack and zero lift. The nose angle was fixed at 6 deg. The length of the body is 150 ft with the cross-sectional radius at the end fixed at 7.8828 ft with a 0-deg slope. The bounds on cross-sectional radii and z-station locations (r, z) were set at $\pm 2\%$ of the initial design. To reduce the overall complexity of the problem, FEM shells have been used, as opposed to a detailed truss structure on which a "skin" is attached. The use of shells, however, results in a lower deformation from the aeroelastic loads than would be the case for a truss structure. Consequently, structural material properties were artificially chosen to allow the structure to demonstrate significant static aeroelastic response for the given flow condition.

The structural shape optimization forms the last two steps of the proposed three-step approach. Step 2 determines an optimal shell thickness, which satisfies the desired maximum nodal deflection requirement, and step 3 finds the optimal jig shape. For this example, the desired maximum nodal deflection Δ_D was 0.5 ft. For step 2 the weighting factors W_1 and W_2 in Eq. (3) were set to 1 and 10, respectively, ensuring the second term drove the optimization. The results from step 2 yielded an objective function value $f_2^{fin} = 0.112$ from an initial value of $f_2^{ini} = 1.0122$ in 180 function evaluations. This corresponded to an optimal thickness of 0.3559 ft and a maximum nodal deflection of 0.5017 ft or 0.34% difference from the desired maximum deflection. This design represents an average 0.095-ft difference between the actual and the desired deflected shape at each nodal location.

The structural shape optimization in step 3 was initiated from the optimal solution found after step 2. It employed a modified objective function as shown in Eq. (4):

$$\min f_3(r, z, t) = \left(\frac{1}{50} \sum_{i=1}^{50} \delta_i^2 + |\Delta_D - \Delta_A| \right)^{\frac{1}{2}} \qquad (4)$$

This formulation gives equal weight to both terms during the optimization process. Step 3 produced an objective function value $f_3^{fin} = 0.0470$ ft from $f_3^{ini} = 0.0942$ ft in 150 function evaluations. The optimal thickness was 0.3484 ft giving a maximum nodal deflection of 0.5112 ft or 2.24% higher than the desired maximum. This final design represents an average 0.045-ft difference between the actual and the desired deflected shape at each nodal location, or a 52% improvement from the design found at the end of step 2.

As no aerodynamic analyses are done throughout the structural shape optimization, verification of the drag for the final jig-shape incorporating aeroelastic effects is necessary. Using a standard direct iterative scheme, that is, alternating between aerodynamic and structural analyses, the coefficients of drag for the undeflected and deflected shapes were determined to be 0.009901 and 0.009065, respectively, an 8.44% reduction. The coefficient of drag for the deflected jig shape was 5.2% lower than that of the desired deflected body ($C_d = 0.009565$).[14] As results from the first phase, aerodynamic shape optimization, are near-optimal solutions, bodies with slightly improved aerodynamic performance after the second phase are possible, as is the case here.

This simple forebody example illustrates that true decoupling of the jig-shape problem, and the use of high-fidelity codes is possible. The use of the stochastic optimizer eliminates the need to evaluate gradients, a process that can require considerable computational resources for problems with a relatively large number of design variables.

HSCT Wing Design Problem

The second example looked at the aeroelastic design of an HSCT wing. The baseline HSCT configuration obtained from NASA Langley (Fig. 5) was assumed to be S_{dd}. The wing body had a coefficient of drag $C_d = 0.00766$. For this example the fuselage and a portion of the wing body from the centerline out to the end of the left span was omitted. The resulting wing (Fig. 6) had an area of 4373 ft^2, a leading-edge sweep of 74 deg inboard and 45 deg outboard, and a wing span of 73.23 ft. The geometry of the wing was defined at five different cross sections along the span, each cross section defined by 20 points. The FEM model had 200 elements. As in the forebody example, material properties were chosen to allow the structure to demonstrate an exaggerated static aeroelastic response

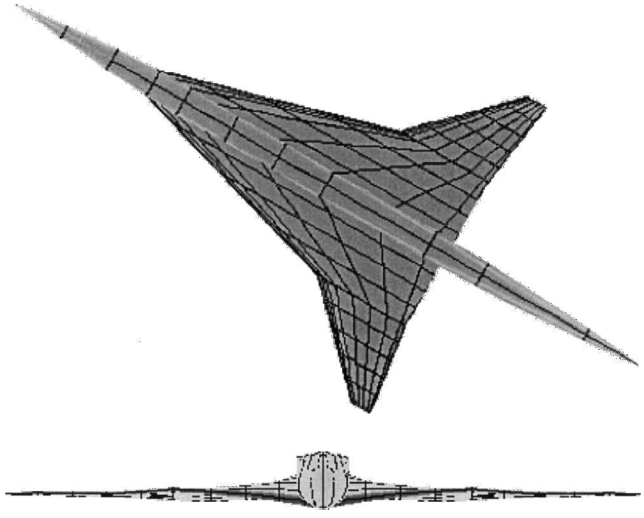

Fig. 5 Typical HSCT configuration.

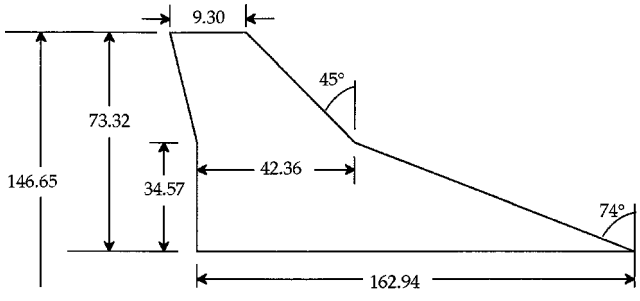

Fig. 6 HSCT baseline wing.

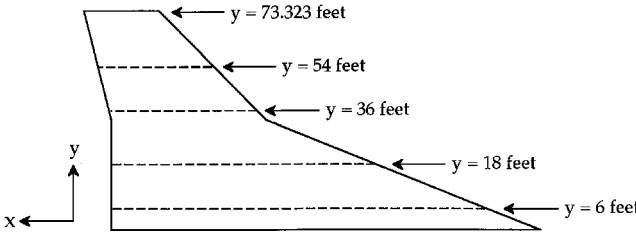

Fig. 7 Locations of the five stations along the span where the design variables are defined.

for the given flow conditions. This is because shell elements were used in the FEM, as opposed to an underlying truss with a metallic "skin."

The profiles of the cross sections of the airfoil at each of the stations were assumed fixed, limiting in-plane deformations to rigid-body translations and rotations. New wing configurations were approximately modeled with an equivalent vertical translation (wing shear) and twist angle at five span locations approximately 18 ft apart (Fig. 7), yielding 10 design variables. A cubic spline that forms the leading edge was defined by the wing shear design variables, whereas the trailing edge was defined by five twist angle design variables. Because the airfoil cross sections were assumed constant, the remaining geometry could be interpolated between the leading and trailing edges.

The desired aerodynamic loading was calculated at flight conditions of Mach 2.4 at 55,000 ft with a 4-deg angle of attack. These loads were transferred from the fluids mesh by interpolation onto the corner nodes of the 200 FEM model elements of the wing. The nodes corresponded to the geometrical points used to define the shape of the wing. In an effort to reduce the computational expense, the design space was discretized, thereby reducing the number of possible body configurations. Throughout the optimization the first

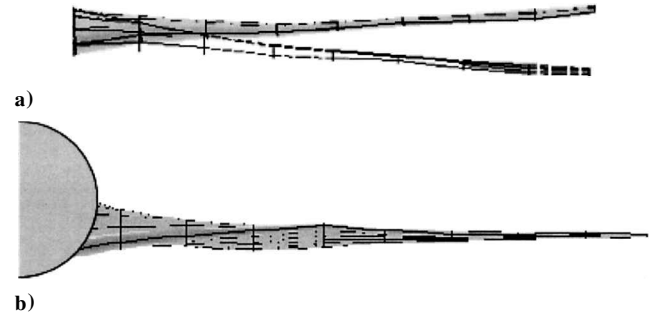

Fig. 8 Rear view of a) the undeflected (unshaded) and the deflected jig shape and b) the desired deflected shape.

20 elements on the farthest inboard portion of the wing were ignored as that part of the wing inside the fuselage and does not affect aerodynamic performance.

There is a great deal of difficulty in numerically comparing two three-dimensional surfaces. As this study served as a proof-of-concept, the comparison was achieved by measuring the difference between the centroids of the desired and deflected body elements. Future investigations will look at more accurate representations.

In the first step of the shape optimization process, the weights W_1 and W_2 in Eq. (2) were set to 0.1 and 50, respectively, and a desired maximum deflection Δ_D was set to 10% of the wing span or 7.332 ft. These values for the weights were found iteratively. It took about 6 or 7 attempts before we were satisfied that the weights were satisfactory for the optimization process. The optimization run yielded an objective function $f_2^{fin} = 3.549$ from an initial value of $f_2^{ini} = 288.371$ in 110 function evaluations. This gave an optimal shell thickness of $t = 0.1853$ ft corresponding to a maximum deflection of 7.283 ft, a 0.67% difference with the Δ_D. This design corresponded to a 0.1904-ft difference between the S_{dd} and S_{ad} at each of the 200 element centroids.

Using this solution as the starting point for step 3 and weights of 1 and 50, respectively, an optimal solution of $f_2^{fin} = 26.7429$ was calculated from an initial value of $f_2^{ini} = 34.281$ in 130 function evaluations. The optimal shell thickness was found to be $t = 0.1896$ ft, yielding an actual maximum deflection of 7.0878 ft, a 3.3% difference from the desired. This final design corresponded to an average 0.1483-ft difference between S_{dd} and S_{ad} at each of the 200 element centroids, or a 22% improvement from the solution obtained in the first step. Figure 8a illustrates the deflected and undeflected shape of the final design. Figure 8b displays the desired deflected shape.

The small geometric difference between the S_{dd} and S_{ad} at each of the 200 element centroids showed that satisfactory results could be obtained by this approach, despite the use of only 10 design variables and a coarse geometry, both insufficient to exactly model the geometry of the undeflected wing. Higher accuracy could be achieved by defining the geometry at more spanwise and chordwise locations. This example also demonstrates that the use of high-fidelity codes to perform the analyses is feasible. For this study aeroelastic drag was not computed for the final design. Future work, where the geometry is more accurately defined, will also include full static aeroelastic verification of the final design.

Conclusions

A novel decoupled approach to the jig-shape aeroelastic wing design problem is presented in this paper. The aerodynamic and structural shape optimizations are performed independently and sequentially. Unlike previous approaches, no aerodynamic analyses need to be performed during the shape optimization. This results in a significant reduction in the required computational resources and makes the use of high-fidelity codes viable.

Because computational cost and organizational difficulties often limit the implementation of MDO procedures for aeroelastic design, approximations are typically employed whereby the optimizer is applied to a sequence of approximate problems. Although

approximation methods play a significant role in the preliminary design process, higher-fidelity codes are needed to provide accurate, detailed analyses of static aeroelastic phenomena. With two manageable yet significant optimization problems, this investigation has demonstrated the feasibility of employing a decoupled jig-shape approach to static aeroelastic design.

Designing for the cruise condition is just one of many, often competing, criteria in any multidisciplinary/multicriteria design optimization problem. Typically, multiple objective functions must be evaluated and a compromise solution sought defining the optimal design. The approach presented in this paper can be incorporated into any MDO strategy where one of the design goals is minimizing drag at the cruise condition.

Acknowledgment

This work was supported by NASA Langley Research Center, Hampton, Virginia, under Grant MBO NAG-1-1559.

References

[1]Bhatia, K. G., and Wertheimer, J., "Aeroelastic Challenges for a High Speed Civil Transport," *34th AIAA/ASME/ASCE/AHS/ASC Structures, Structural Dynamics and Materials Conference*, AIAA Paper 93-1478, AIAA, Washington, DC, April 1993, pp. 3661–3682.

[2]Baker, M., and Giesing, A., "A Practical Approach to MDO and its Applications to an HSCT Aircraft," AIAA Paper 95-3885, Sept. 1995.

[3]Chattopadhyay, A., and Pagaldipti, N., "A Multidisciplinary Optimization Using Semi-Analytical Sensitivity Analysis Procedure and Multilevel Decomposition," *Journal of Computers and Mathematics with Applications*, Vol. 29, No. 7, 1995, pp. 55–66.

[4]Sobieszczanski-Sobieski, J., and Haftka, R., "Multidisciplinary Aerospace Design Optimization: Survey of Recent Developments," *34th Aerospace Sciences Meeting and Exhibit*, AIAA Paper 96-0711, AIAA, Reston, VA, Jan. 1996, pp. 1–33.

[5]Rohl, P. J., Mavris, D. N., and Schrage, D. P., "Combined Aerodynamic and Structural Optimization of High Speed Civil Transport Wing," *36th AIAA/ASME/ASCE/AHS/ASC Structures, Structural Dynamics and Materials Conference*, AIAA Paper 95-1222, AIAA, Washington, DC, April 1995, pp. 548–557.

[6]Raveh, D., and Karpel, M., "Structural Optimization of Flight Vehicles with Computational-Fluid-Dynamics-Based Maneuver Loads," *Journal of Aircraft*, Vol. 36, No. 6, 1998, pp. 1007–1015.

[7]Garcelon, J., Balabanov, V., and Sobieski, J., "Multidisciplinary Optimization of a Transport Aircraft Wing Using VisualDOC," *AIAA/ASME/ASCE/AHS/ASC Structures, Structural Dynamics and Materials Conference*, AIAA Paper 99-1349, AIAA, Reston, VA, April 1999, pp. 1306–1313.

[8]Karpel, M., Moulin, B., and Love, M., "Modal-Based Structural Optimization with Static Aeroelastic and Stress Constraints," *AIAA/ASME/ASCE/AHS/ASC Structures, Structural Dynamics and Materials Conference*, AIAA, Reston, VA, 1996, pp. 1494–1503; *Journal of Aircraft*, Vol. 34, No. 3, 1997, pp. 433–440.

[9]Karpel, M., Moulin, B., and Love, M., "Structural Optimization with Static Aeroelastic and Stress Constraints Using Expandable Modal Basis," *AIAA Journal*, Vol. 37, No. 11, 1999, pp. 1514–1519.

[10]Huang, X., Dudley, J., Haftka, R. T., Grossman, B., and Mason, W., "Structural Weight Estimation of Multidisciplinary Optimization of High Speed Civil Transport," *Journal of Aircraft*, Vol. 33, No. 3, 1996, pp. 608–616.

[11]McCullers, L. A., Flight Optimization System, Computer Program and Users Guide, Ver. 5.7., NASA Langley Research Center, Hampton, VA, 1994.

[12]Neill, D. J., and Herendeen, D. L., "Automated Structural Optimization System (ASTROS)," U.S. Air Force Wright Aeronautical Lab., TR-93-3025, Dayton, OH, 1993.

[13]Aly, S., Marconi, F., Ogot, M., Pelz, R., and Siclari, M., "Stochastic Optimization Applied to CFD Design," AIAA Paper 95-1647, Jan. 1995.

[14]Aly, S., Ogot, M., and Pelz, R., "A Stochastic Approach to Optimal Aerodynamic Shape Design," *Journal of Aircraft*, Vol. 33, No. 5, 1996, pp. 956–961.

[15]Farhat, C., Lesoinne, M., and Koobus, B., "A High Fidelity and High Performance Computational Methodology for the Solution of Transient Nonlinear Viscous Aeroelastic Problems," *1st AFOSR Conference on Dynamic Motion CFD*, edited by L. Sakell and D. D. Knight, AFSOR, Arlington, VA, 1996, pp. 159–187.

[16]Maman, N., and Farhat, C., "Matching Fluids and Structure Meshes for Aeroelastic Computations: A Parallel Approach," *Computers and Structures*, Vol. 54, No. 4, 1995, pp. 779–785.

[17]Blair, M., "A Unified Aeroelastic Surface Formulation," *35th AIAA/ASME/ASCE/AHS/ASC Structures, Structural Dynamics and Materials Conference*, Hilton Head, SC, Vol. 3, April 1994, pp. 1276–1283.

[18]Bhardwaj, M. K., Kapania, R. K., Reichenbach, E., and Guruswamy, G. P., "Computational Fluid Dynamics/Computational Structural Dynamics Interaction Methodology for Aircraft Wings," *AIAA Journal*, Vol. 36, No. 12, 1998, pp. 2179–2186.

[19]Samareh, J., "Use of CAD Geometry in MDO," *6th AIAA/NASA/ISSMO Symposium on Multidisciplinary Analysis and Optimization*, AIAA Paper 96-3991, AIAA, Reston, VA, Sept. 1996, pp. 88–97.

[20]Gupta, K., "Development of a Finite Element Aeroelastic Analysis Capability," *Journal of Aircraft*, Vol. 33, No. 5, 1996, pp. 995–1001.

[21]Newman, J., III, Newman, P., Taylor, A., and Houc, G., "Efficient Nonlinear Static Aeroelastic Wing Analysis," *Computers and Fluids*, Vol. 28, No. 4, 1999, pp. 615–628.

[22]Byun, C., and Guruswamy, G., "Wing-Body Aeroelasticity on Parallel Computers," *Journal of Aircraft*, Vol. 33, No. 2, 1996, pp. 421–428.

[23]Smith, M., Hodges, D., and Cesnik, C., "Evaluation of Computational Algorithms Suitable for Fluid-Structure Interactions," *Journal of Aircraft*, Vol. 33, No. 2, 2000, pp. 282–294.

[24]Siclari, M., and Del Guidice, P., "A Multigrid Finite Volume Method for Solving the Euler and Navier–Stokes Equations for High Speed Flows," AIAA Paper 89-0283, Jan. 1989.

[25]Siclari, M., and Del Guidice, P., "Hybrid Finite Element Volume Approach to Euler Solutions for Supersonic Flows," *AIAA Journal*, Vol. 28, No. 1, 1990, pp. 66–74.

[26]Siclari, M., and Darden, C. M., "CFD Predictions of the Near-Field Sonic Boom Environment for Two Low Boom HSCT Configurations," AIAA Paper 91-1631, June 1991.

[27]*ANSYS 5.2 User's Manual*, Swanson Analysis Systems, Houston, PA, 1995.